Electronic Research Archive

http://www.aimspress.com/journal/era

ERA, 30(12): 4530–4552.
DOI: 10.3934/era.2022230
Received: 15 February 2022
Revised: 04 June 2022
Accepted: 09 June 2022
Published: 17 October 2022

Research article

Controlled dynamics of a chemotaxis model with logarithmic sensitivity by physical boundary conditions

Ling Xue[1,*], **Min Zhang**[1], **Kun Zhao**[2] **and Xiaoming Zheng**[3]

[1] College of Mathematical Sciences, Harbin Engineering University, Harbin 150001, China
[2] Department of Mathematics, Tulane University, LA 70118, USA
[3] Department of Mathematics, Central Michigan University, MI 48859, USA

* **Correspondence:** Email: lxue@hrbeu.edu.cn.

Abstract: We study the global dynamics of large amplitude classical solutions to a system of balance laws, derived from a chemotaxis model with logarithmic sensitivity, subject to time-dependent boundary conditions. The model is supplemented with H^2 initial data and unmatched boundary conditions at the endpoints of a one-dimensional interval. Under suitable assumptions on the boundary data, it is shown that classical solutions exist globally in time. Time asymptotically, the differences between the solutions and their corresponding boundary data converge to zero, as time goes to infinity. No smallness restrictions on the magnitude of the initial perturbations is imposed. Numerical simulations are carried out to explore some topics that are not covered by the analytical results.

Keywords: chemotaxis; dynamic boundary conditions; large data solution; long-time behavior

1. Introduction

1.1. Background

This paper focuses on the boundary control of large amplitude classical solutions to an initial-boundary value problem of the system of hyperbolic balance laws:

$$u_t - (uv)_x = u_{xx}, \tag{1.1a}$$
$$v_t - (u^\gamma - v^2)_x = v_{xx}, \tag{1.1b}$$

which originates from the chemotaxis model with logarithmic sensitivity:

$$u_t = Du_{xx} - \chi\big[u(\log c)_x\big]_x, \tag{1.2a}$$
$$c_t = \varepsilon c_{xx} - \mu u^\gamma c. \tag{1.2b}$$

Chemotaxis is the biochemical process through which the movement of an organism or entity is not only regulated by random diffusion, but also controlled by the concentration gradient of a chemical stimulus in the local environment. Biological processes undergoing chemotaxis include bacterial foraging, immune response, embryonic development and tissue homeostasis [1,2], blood vessel formation [3], fish pigmentation patterning [4], tumor angiogenesis [5], primitive streak formation [6], slime mould formation [7], and wound healing [8], just to name a few.

Interpretation of the underlying mechanism of chemotaxis using continuum PDE models dates bak to the 1950s by Patlak [9] and the 1970s by Keller and Segel [10–12], the former from a probabilistic perspective, and the latter based on a phenomenological approach. In a general form, the Patlak-Keller-Segel model can be expressed as

$$u_t = Du_{xx} - \chi[u\,\Phi(c)_x]_x, \tag{1.3a}$$
$$c_t = \varepsilon c_{xx} + f(u, c), \tag{1.3b}$$

which is a system of reaction-diffusion-advection equations. Here, the unknown functions $u(x, t)$ and $c(x, t)$ denote the density of the organic population and concentration of the chemical signal at position x at time t, respectively. The parameters: $D > 0$ stands for the diffusion coefficient of the organic density; $\chi \neq 0$ is the coefficient of chemotactic sensitivity, the sign of χ dictates whether the chemotaxis is attractive ($\chi > 0$) or repulsive ($\chi < 0$), with $|\chi|$ measuring the strength of chemotactic response; and $\varepsilon \geq 0$ is the diffusion coefficient of the chemical signal. The function $\Phi(c)$ denotes the chemotactic sensitivity, which underlines the main character of such a model, whose spatial derivative depicts the mechanistic feature of chemotactic movement – advection of the organic population induced by the spatial gradient of the chemical signal in the local environment. Moreover, the function $f(u, c)$ accounts for consumption/production/degradation of the chemical signal. Formally, the model portrays the evolution (biased movement) of the organic population in response to the chemical stimulus in the local environment. Mathematically, the synergy of random diffusion, nonlinear advection and nonlinear reaction makes the dynamics of the model an intriguing problem to investigate. Depending on the specific forms of $\Phi(c)$ and $f(u, c)$, the model can be utilized to explain the underlying mechanisms of various biological processes experiencing chemotaxis. We refer the readers to the survey papers [13–15] for a comprehensive list and the mathematical development of such models.

To introduce the specific problem, we first present the following model, which is a special version of (1.3) when Φ is the logarithmic function of c and $f(u, c)$ is a polynomial of u and c:

$$u_t = Du_{xx} - \chi[u\log(c)_x]_x, \tag{1.4a}$$
$$c_t = \varepsilon c_{xx} - \mu uc - \sigma c, \tag{1.4b}$$

where the parameter $\mu \neq 0$ denotes the density-dependent production/degradation rate of the chemical signal and $\sigma \geq 0$ stands for the natural degradation rate of the chemical signal. When $\sigma = 0$, this model can be viewed as a borderline case of one of the original models developed by Keller and Segel:

$$u_t = Du_{xx} - \chi[u\log(c)_x]_x, \tag{1.5a}$$
$$c_t = \varepsilon c_{xx} - \mu uc^m, \qquad 0 \leq m < 1, \tag{1.5b}$$

which appeared in [12] to understand J. Adler's experimental result [16] on the formation of traveling bands in nutrient-enticed *E. Coli* population. The logarithmic sensitivity entails that the chemotactic movement obeys the Weber-Fechner's law, which is a fundamental principle in psychophysics and has prominent applications in biology ([12, 17–20]).

System (1.4) appeared in a variety of contexts to elucidate the fundamental principles of different chemotactic processes. For example, when $\chi < 0$, $\mu < 0$ and $\sigma > 0$, the model was designed in [21,22] to illustrate the chemotactic movement of reinforced random walkers, such as surface or matrix-bound adhesive molecules, which deposit non-diffusive ($\varepsilon = 0$) or slowly moving ($0 < \varepsilon \ll 1$) chemical signals that modify the local environment for succeeding passages. In light of the biological contexts of the parameters χ and μ, the model characterizes the process of repulsive chemotaxis in response to a chemical stimulus that is being produced by the organism. On the other hand, when $\chi > 0$, $\mu > 0$ and $\sigma = 0$, the model was employed by Levine et al. [23] to interpret the dynamical interactions between vascular endothelial cells (VECs) and signaling molecules vascular endothelial growth factor (VEGF) in the onset of tumor angiogenesis. In this case, the model portrays the process of attractive chemotaxis in response to a chemical stimulus that is being consumed by the organism.

It should be stressed that although the logarithmic sensitivity plays an important role in biological modeling, its singular nature brings out an obstruction for the qualitative (numerical and rigorous) analysis of the mathematical equations. The existing results concerning the qualitative behavior of the models with logarithmic sensitivity is much less than those with other types of sensitivity, such as linear sensitivity, saturating sensitivity, et al, see e.g., [13–15]. Fortunately, it has been recognized that the singular nature of the logarithmic sensitivity can be removed by applying the Cole-Hopf type transformation: $v = \left[\log(e^{\sigma t}c)\right]_x = \frac{c_x}{c}$. Combining such a transformation with the temporal-spatial rescaling:

$$t \to |\chi\mu| D^{-1}\, t, \quad x \to \sqrt{|\chi\mu|}\, D^{-1}\, x, \quad v \to -\text{sign}(\chi)\sqrt{|\chi|\,|\mu|^{-1}}\, v,$$

one can convert the original chemotaxis model into

$$u_t - (uv)_x = u_{xx}, \tag{1.6a}$$

$$v_t - \text{sign}(\chi\mu)u_x = \varepsilon D^{-1} v_{xx} - \varepsilon\chi^{-1}(v^2)_x, \tag{1.6b}$$

where the equations are written in the conservative form to facilitate further discussions in the context of balance laws. A direct calculation shows that the characteristics associated with the flux in (1.6) are

$$\lambda_\pm = \frac{\left(2\varepsilon\chi^{-1} - 1\right)v \pm \sqrt{\left(2\varepsilon\chi^{-1} + 1\right)^2 v^2 + 4\,\text{sign}(\chi\mu)u}}{2}, \tag{1.7}$$

from which we see that the principle part of (1.6) is hyperbolic in biologically relevant regimes (where the cellular density $u > 0$), provided $\chi\mu > 0$. Hence, the analytical tools in hyperbolic balance laws become feasible for studying the qualitative behavior of the model. We focus on this case throughout the paper, since otherwise the characteristic fields may change the type, which could alter the dynamics of the model drastically. This is supported by the finite-time blowup of the explicit and numerical solutions constructed in [21].

Rigorous mathematical study of (1.6) has been carried out for nearly two decades. Most of the results are established for the case when $\chi\mu > 0$. The global well-posedness of large amplitude classical solutions was first established in [24, 25], and upgraded in a series of recent works [26–35] under

various initial and/or boundary conditions. The existence and local stability of large-strength traveling waves and boundary spike-layer solutions have been settled in [36–44] and [45], respectively. There are also works investigating the qualitative behavior of the appended version of (1.6) with logistic growth [46–51]. Collectively, these results suggest that large-time homogenization is generic in the processes of logarithmically sensitive chemo-attraction with chemical consumption and chemo-repulsion with chemical production, while finite-time singularities are not expected in such processes.

Inspired by the biological background and the mathematical research recently conducted on (1.6), the following model was proposed and analyzed in [52, 53]:

$$u_t = Du_{xx} - \chi[u(\log c)_x]_x, \tag{1.8a}$$

$$c_t = \varepsilon c_{xx} - \mu u^\gamma c - \sigma c, \qquad \gamma > 1, \tag{1.8b}$$

which is an amended version of (1.4) by replacing the linear dependence of the chemical production/consumption rate on the organic density by a power-like one. Since monomials are building blocks of general nonlinear functions, this model paves a way for the understanding of the dynamical behavior of the Keller-Segel type model with genuinely nonlinear production/consumption rates. By applying the Cole-Hopf transformation and the rescaling applied to (1.4), we obtain

$$u_t - (uv)_x = u_{xx}, \tag{1.9a}$$

$$v_t - \mathrm{sign}(\chi\mu)(u^\gamma)_x = \varepsilon D^{-1} v_{xx} - \varepsilon\chi^{-1}(v^2)_x, \tag{1.9b}$$

which is the focal point of this paper. From the perspective of rigorous mathematical analysis, (1.9) is considerably more complicated than (1.6), due to the power-like nonlinearity. So far, the global stability of constant ground states and convergence rates in the regime of classical solutions to the Cauchy problem has been proven in [53, 54], and the global stabilization of classical solutions on finite intervals subject to dynamic boundary conditions has been demonstrated in [52].

1.2. Motivation

Mathematically, the initial-boundary value problem of a PDE model subject to dynamic (time-dependent) boundary conditions can be equivalently viewed as a control problem with the boundary data as external inputs. A typical question in this type of problem is under what conditions on the boundary data the solution stabilizes in the long run. Such a problem has been studied for (1.9) in [52], where the global stabilization of large data classical solutions under dynamic boundary conditions is established. However, we note that the result of [52] required the boundary values of the unknown functions to match at the endpoints, i.e., $u(a,t) = u(b,t)$ and $v(a,t) = v(b,t)$. Apparently, such a restriction is not desirable from the physical/biological point of view. Rigorous mathematical study of the models subject to *unmatched* boundary conditions, i.e., $u(a,t) \neq u(b,t)$ and $v(a,t) \neq v(b,t)$, thus becomes physically/biologically relevant. Nevertheless, the long-time dynamics of large data solutions to the model subject to unmatched boundary conditions still remains to be investigated. This has been highlighted in Remark 1.1 of [52]. To enrich the contemporary body of knowledge, we dedicate this paper to the investigation of such a problem. Since γ serves as a tuning parameter and the dynamic boundary data are regarded as external inputs, our major task is to identify the conditions on the parameter value and the boundary data, under which solutions to the initial-boundary value problem of the model stabilize when time getting large. Comparing with the case of matched boundary

data, the analysis under unmatched boundary conditions is much more involved, since the reference profile depends on the spatial variable. Hence, the combined effect of the spatially dependent reference profile coupled with power-like/quadratic nonlinearities creates an intriguing mathematical problem to pursue.

1.3. Statement of results

To simplify the presentation, we take $\chi = D = \varepsilon = 1$, since the specific values of the parameters do not affect the underlying analysis. Also, recall that we are focusing on the case when $\chi\mu > 0$. Under these circumstances, we obtain the cleaner version of (1.9):

$$u_t - (uv)_x = u_{xx}, \tag{1.10a}$$
$$v_t - (u^\gamma)_x = v_{xx} - (v^2)_x, \qquad \gamma > 1. \tag{1.10b}$$

The system is supplemented with the initial conditions

$$(u, v)(x, 0) = (u_0, v_0)(x), \quad x \in [0, 1], \tag{1.11}$$

and the boundary conditions:

$$u(0, t) = \alpha_1(t), \quad u(1, t) = \alpha_2(t), \quad t \geq 0, \tag{1.12a}$$
$$v(0, t) = \beta_1(t), \quad v(1, t) = \beta_2(t), \quad t \geq 0. \tag{1.12b}$$

The main result of this paper addresses the global nonlinear stability of large data classical solutions to (1.10) when $\gamma = 2$ and subject to unmatched dynamic boundary conditions.

Theorem 1.1. *Consider the initial-boundary value problems* (1.10)–(1.12) *with* $\gamma = 2$. *Suppose the initial data satisfy* $u_0 > 0$, $(u_0, v_0) \in [H^2((0, 1))]^2$, *and are compatible with the boundary conditions. Assume* α_1, α_2, β_1, *and* β_2 *are smooth functions on* $[0, \infty)$, *and satisfy the following conditions:*

- $\alpha_1(t) \geq \underline{\alpha}_1 > 0, \quad \alpha_2(t) \geq \underline{\alpha}_2 > 0, \quad \forall\, t \geq 0,$ (1.13)
- $\alpha_1 - \alpha_2 \in L^1((0, \infty)) \quad \textit{and} \quad \alpha_1', \alpha_2' \in W^{1,1}((0, \infty)),$ (1.14)
- $\beta_1 - \beta_2 \in L^1((0, \infty)) \quad \textit{and} \quad \beta_1', \beta_2' \in W^{1,1}((0, \infty)),$ (1.15)

where $\underline{\alpha}_i$ *are constants. Then there exists a unique solution to the IBVP, such that*

$$\|\tilde{u}(t)\|^2_{H^2((0,1))} + \|\tilde{v}(t)\|^2_{H^2((0,1))} + \int_0^t (\|\tilde{u}(\tau)\|^2_{H^3((0,1))} + \|\tilde{v}(\tau)\|^2_{H^3((0,1))}) \mathrm{d}\tau \leq C,$$

where

$$\tilde{u}(x, t) = u(x, t) - \alpha(x, t), \quad \alpha(x, t) = [\alpha_2(t) - \alpha_1(t)]x + \alpha_1(t),$$
$$\tilde{v}(x, t) = v(x, t) - \beta(x, t), \quad \beta(x, t) = [\beta_2(t) - \beta_1(t)]x + \beta_1(t),$$

and the constant $C > 0$ *is independent of* t. *Moreover, the solution obeys the long-time behavior*

$$\|\tilde{u}(t)\|^2_{H^2((0,1))} + \|\tilde{v}(t)\|^2_{H^2((0,1))} \to 0 \quad \textit{as} \quad t \to \infty.$$

We have the following remarks concerning Theorem 1.1.

Remark 1.1. *Since we did not specify any decay rate for the boundary data, the rate of convergence of the perturbed functions can not be identified under the assumptions of Theorem 1.1. The integrability conditions of the boundary data present general criteria that guarantee the convergence of the perturbations. On the other hand, if we specify certain decay rates for α_i and β_i, then the convergence rate of $\tilde{u}$ and $\tilde{v}$ could be determined by using ODE arguments. We refer the reader to the example in the Appendix of [55], whose proof can be adapted to fit into the situation encountered in this paper.*

Remark 1.2. *The technical assumptions in Theorem 1.1 imply the difference between the corresponding boundary data will converge to zero as $t \to \infty$, i.e., the unmatched boundary data will eventually match. However, based on the assumptions we see that the boundary functions do not necessarily equal to each other at any finite time. In addition, there is no smallness restriction on the amplitude of the initial perturbation around the reference profile.*

Remark 1.3. *Since the boundary data are smooth functions on $[0, \infty)$ and their first order derivatives belong to $W^{1,1}((0, \infty))$, it follows from the Fundamental Theorem of Calculus that the functions themselves and their first order derivatives are uniformly bounded with respect to t. Such information will be frequently utilized in the proof of the theorem.*

Remark 1.4. *Our result only covers a single value of γ, i.e., $\gamma = 2$. For other values of γ, it is not clear whether similar results hold true or not. We provide numerical results towards the end of the paper to present some positive evidences, while leave the rigorous investigation for future work. On the other hand, we would like to mention that by combining the analysis of this paper with the techniques in [33], especially the Orlicz-type free energy functional, one can establish a similar result for the original model* (1.6) *under the boundary conditions: $u(0, t) = u(1, t) = \alpha(t)$, $v(0, t) = \beta_1(t)$, $v(1, t) = \beta_2(t)$, where $\beta_1(t) \neq \beta_2(t)$, and α, β_1, β_2 satisfy similar conditions as those in Theorem 1.1. However, the problem with unmatched boundary data for $u(x, t)$ can not be settled at this point, due to technical obstructions caused by the Orlicz-type functional. We also leave the investigation for future work.*

We prove Theorem 1.1 in Section 2. The proof is self-contained, utilizing delicate energy methods. We apply various elementary inequalities, such as Cauchy-Schwarz, Young, Hölder and Grönwall. The energy estimates are carefully crafted to unveil the assumptions about the growth/decaying properties of the boundary data. In Section 3, we present numerical results to illustrate some problems that are not covered by Theorem 1.1, including dynamic boundary data with non-trivial final profiles, time periodic boundary conditions, and the case when γ is a fraction. For notational convenience, throughout the rest of the paper, we use $\|\cdot\|$ and $\|\cdot\|_\infty$ to denote the standard norms $\|\cdot\|_{L^2}$ and $\|\cdot\|_{L^\infty}$, respectively. The functional space $H^s((0, 1))$ is denoted by H^s. Moreover, we use C to denote a generic constant which is independent of time, but may depend on the initial and/or boundary data. The value of the constant may vary line by line according to the context.

2. Proof of Theorem 1.1

We now prove Theorem 1.1. The proof is divided into several steps which are contained in a series of subsections. We define the reference profiles:

$$\alpha(x,t) = [\alpha_2(t) - \alpha_1(t)]x + \alpha_1(t),$$
$$\beta(x,t) = [\beta_2(t) - \beta_1(t)]x + \beta_1(t),$$

which interpolate the boundary data in the linear fashion. To facilitate the asymptotic analysis, we let

$$\tilde{u}(x,t) = u(x,t) - \alpha(x,t),$$
$$\tilde{v}(x,t) = v(x,t) - \beta(x,t).$$

In terms of $\tilde{u}$ and $\tilde{v}$, system (1.10) with $\gamma = 2$ reads as

$$\tilde{u}_t - (\tilde{u}\tilde{v})_x = \tilde{u}_{xx} + (\alpha\tilde{v})_x + (\beta\tilde{u})_x + (\alpha\beta)_x - \alpha_t, \tag{2.1a}$$
$$\tilde{v}_t - (\tilde{u}^2)_x = \tilde{v}_{xx} - (\tilde{v}^2)_x - 2(\beta\tilde{v})_x - (\beta^2)_x + 2(\alpha\tilde{u})_x + (\alpha^2)_x - \beta_t, \tag{2.1b}$$

with the initial and boundary conditions

$$\text{I.C.} \qquad (\tilde{u},\tilde{v})(x,0) = (u_0(x) - \alpha(x,0), v_0(x) - \beta(x,0)), \quad x \in [0,1], \tag{2.2}$$
$$\text{B.C.} \qquad \tilde{u}(0,t) = \tilde{u}(1,t) = 0, \quad \tilde{v}(0,t) = \tilde{v}(1,t) = 0, \quad t \geq 0. \tag{2.3}$$

First of all, under the assumptions of Theorem 1.1, the local well-posedness of solutions to (2.1), (2.2) and (2.3) can be established by using standard approaches, such as Galerkin approximation and fixed point argument, along with the energy estimates derived in this section. We present the result without going through the technical details in order to simplify the presentation.

Lemma 2.1. *Under the assumptions of Theorem* 1.1*, there exist a finite $T_0 > 0$ and a unique solution $(\tilde{u},\tilde{v})$ to* (2.1)*,* (2.2) *and* (2.3)*, such that $(\tilde{u},\tilde{v}) \in \left[C([0,T_0];H^2) \cap L^2(0,T_0;H^3)\right]^2$.*

Next, we shall derive the *a priori* estimates of the local solution, in order to extend it to a global one. The *a priori* estimates alongside their proofs are recorded in the following subsections.

2.1. $L_t^\infty L_x^2$–$L_t^2 H_x^1$–Estimates

Lemma 2.2. *Under the assumptions of Theorem* 1.1*, there exists a constant $C > 0$ which is independent of t, such that*

$$\|\tilde{u}(t)\|^2 + \|\tilde{v}(t)\|^2 + \int_0^t (\|\tilde{u}_x(\tau)\|^2 + \|\tilde{v}_x(\tau)\|^2)\mathrm{d}\tau \leq C.$$

Proof. Taking L^2 inner product of (2.1a) with $2\tilde{u}$ and integrating by parts, we can show that

$$\frac{\mathrm{d}}{\mathrm{d}t}\|\tilde{u}\|^2 + 2\|\tilde{u}_x\|^2 = -2\int_0^1 \tilde{u}\tilde{v}\tilde{u}_x\mathrm{d}x + 2\int_0^1 \alpha_x\tilde{v}\tilde{u}\mathrm{d}x + 2\int_0^1 \alpha\tilde{v}_x\tilde{u}\mathrm{d}x + \int_0^1 \beta_x\tilde{u}^2\mathrm{d}x$$
$$+ 2\int_0^1 (\alpha_x\beta + \alpha\beta_x - \alpha_t)\tilde{u}\mathrm{d}x. \tag{2.4}$$

Taking L^2 inner product of (2.1b) with $\tilde{v}$ and integrating by parts, we can show that

$$\frac{1}{2}\frac{\mathrm{d}}{\mathrm{d}t}\|\tilde{v}\|^2 + \|\tilde{v}_x\|^2 = 2\int_0^1 \tilde{u}\tilde{v}\tilde{u}_x \mathrm{d}x - \int_0^1 \beta_x \tilde{v}^2 \mathrm{d}x - 2\int_0^1 \alpha\tilde{u}\tilde{v}_x \mathrm{d}x + \int_0^1 (2\alpha\alpha_x - 2\beta\beta_x - \beta_t)\tilde{v}\mathrm{d}x. \tag{2.5}$$

Taking the sum of (2.4) and (2.5), we obtain

$$\frac{\mathrm{d}}{\mathrm{d}t}\Big(\|\tilde{u}\|^2 + \frac{1}{2}\|\tilde{v}\|^2\Big) + 2\|\tilde{u}_x\|^2 + \|\tilde{v}_x\|^2 = \underbrace{2\int_0^1 \alpha_x \tilde{v}\tilde{u}\mathrm{d}x}_{\equiv R_{1a}} + \underbrace{\int_0^1 \beta_x \tilde{u}^2 \mathrm{d}x}_{\equiv R_{1b}} \underbrace{- \int_0^1 \beta_x \tilde{v}^2 \mathrm{d}x}_{\equiv R_{1c}} + \underbrace{2\int_0^1 (\alpha_x\beta + \alpha\beta_x - \alpha_t)\tilde{u}\mathrm{d}x}_{\equiv R_{1d}} + \underbrace{\int_0^1 (2\alpha\alpha_x - 2\beta\beta_x - \beta_t)\tilde{v}\mathrm{d}x}_{\equiv R_{1e}}. \tag{2.6}$$

Since $\alpha_x = \alpha_2(t) - \alpha_1(t)$ and $\beta_x = \beta_2(t) - \beta_1(t)$, we infer that

$$|R_{1a}| + |R_{1b}| + |R_{1c}| \le (|\alpha_2 - \alpha_1| + |\beta_2 - \beta_1|)(\|\tilde{u}\|^2 + \|\tilde{v}\|^2).$$

Using the uniform boundedness of α and β, see Remark 1.3, we can show that

$$|R_{1d}| \le (|\alpha_2 - \alpha_1| + |\beta_2 - \beta_1| + |\alpha_2'| + |\alpha_1'|)(1 + \|\tilde{u}\|^2).$$

Similarly, it can be shown that

$$|R_{1e}| \le (|\alpha_2 - \alpha_1| + |\beta_2 - \beta_1| + |\beta_2'| + |\beta_1'|)(1 + \|\tilde{v}\|^2).$$

Substituting the above estimates into (2.6), we can show that

$$\begin{aligned}
&\frac{\mathrm{d}}{\mathrm{d}t}\Big(\|\tilde{u}\|^2 + \frac{1}{2}\|\tilde{v}\|^2\Big) + 2\|\tilde{u}_x\|^2 + \|\tilde{v}_x\|^2 \\
&\le C(|\alpha_2 - \alpha_1| + |\beta_2 - \beta_1| + |\alpha_1'| + |\alpha_2'| + |\beta_1'| + |\beta_2'|)\Big(\|\tilde{u}\|^2 + \frac{1}{2}\|\tilde{v}\|^2\Big) \\
&\quad + C(|\alpha_2 - \alpha_1| + |\beta_2 - \beta_1| + |\alpha_1'| + |\alpha_2'| + |\beta_1'| + |\beta_2'|).
\end{aligned} \tag{2.7}$$

Applying Grönwall's inequality and using the assumptions of Theorem 1.1, we can show that

$$\|\tilde{u}(t)\|^2 + \|\tilde{v}(t)\|^2 + \int_0^t (\|\tilde{u}_x(\tau)\|^2 + \|\tilde{v}_x(\tau)\|^2)\mathrm{d}\tau \le C, \tag{2.8}$$

for some constant which is independent of t. This completes the proof of the lemma. □

2.2. $L_t^\infty H_x^1$–$L_t^2 H_x^2$–Estimates

Lemma 2.3. *Under the assumptions of Theorem* 1.1*, there exists a constant $C > 0$ which is independent of t, such that*

$$\|\tilde{u}_x(t)\|^2 + \|\tilde{v}_x(t)\|^2 + \int_0^t \left(\|\tilde{u}_{xx}(\tau)\|^2 + \|\tilde{v}_{xx}(\tau)\|^2\right) \mathrm{d}\tau \le C.$$

Proof. **Step 1.** Taking L^2 inner product of (2.1a) with $-\tilde{u}_{xx}$, we obtain

$$\begin{aligned}\frac{1}{2}\frac{\mathrm{d}}{\mathrm{d}t}\|\tilde{u}_x\|^2 + \|\tilde{u}_{xx}\|^2 = &\underbrace{-\int_0^1 (\tilde{u}\tilde{v})_x \tilde{u}_{xx}\mathrm{d}x}_{\equiv R_{2a}} \underbrace{-\int_0^1 (\alpha\tilde{v})_x \tilde{u}_{xx}\mathrm{d}x}_{\equiv R_{2b}} \underbrace{-\int_0^1 (\beta\tilde{u})_x \tilde{u}_{xx}\mathrm{d}x}_{\equiv R_{2c}} \\ &\underbrace{-\int_0^1 (\alpha\beta)_x \tilde{u}_{xx}\mathrm{d}x}_{\equiv R_{2d}} + \underbrace{\int_0^1 \alpha_t \tilde{u}_{xx}\mathrm{d}x}_{\equiv R_{2e}}. \end{aligned} \tag{2.9}$$

Applying the Sobolev embedding theorem and Poincaré inequality, we can show that

$$\begin{aligned}|R_{2a}| &\le \|\tilde{u}_x\|\|\tilde{v}\|_\infty\|\tilde{u}_{xx}\| + \|\tilde{u}\|_\infty\|\tilde{v}_x\|\|\tilde{u}_{xx}\| \\ &\le C\|\tilde{u}_x\|\|\tilde{v}_x\|\|\tilde{u}_{xx}\|.\end{aligned}$$

Using the uniform boundedness of $\alpha_x = \alpha_2(t) - \alpha_1(t)$ and α, we deduce

$$\begin{aligned}|R_{2b}| &\le \|\alpha_x\|\|\tilde{v}\|_\infty\|\tilde{u}_{xx}\| + \|\alpha\|_\infty\|\tilde{v}_x\|\|\tilde{u}_{xx}\| \\ &\le C\|\tilde{v}_x\|\|\tilde{u}_{xx}\|.\end{aligned}$$

Similarly, we can show that

$$|R_{2c}| \le C\|\tilde{u}_x\|\|\tilde{u}_{xx}\|.$$

For R_{2d} and R_{2e}, we can show that

$$\begin{aligned}|R_{2d}| &\le (\|\alpha_x\|\|\beta\|_\infty + \|\alpha\|_\infty\|\beta_x\|)\|\tilde{u}_{xx}\| \\ &\le C(|\alpha_2 - \alpha_1| + |\beta_2 - \beta_1|)\|\tilde{u}_{xx}\|,\end{aligned}$$

and

$$|R_{2e}| \le C(|\alpha_2'| + |\alpha_1'|)\|\tilde{u}_{xx}\|,$$

Feeding the above estimates to (2.9), applying Cauchy's inequality, and invoking the uniform boundedness of α, β and their derivatives (see Remark 1.3), we can show that

$$\begin{aligned}&\frac{1}{2}\frac{\mathrm{d}}{\mathrm{d}t}\|\tilde{u}_x\|^2 + \frac{1}{2}\|\tilde{u}_{xx}\|^2 \\ &\le C\|\tilde{u}_x\|^2\|\tilde{v}_x\|^2 + C(\|\tilde{u}_x\|^2 + \|\tilde{v}_x\|^2 + |\alpha_2 - \alpha_1| + |\beta_2 - \beta_1| + |\alpha_1'| + |\alpha_2'|).\end{aligned} \tag{2.10}$$

Applying Grönwall's inequality to (2.10) and utilizing Lemma 2.2, we can show that

$$\|\tilde{u}_x(t)\|^2 + \int_0^t \|\tilde{u}_{xx}(\tau)\|^2 \mathrm{d}\tau \le C, \tag{2.11}$$

where the constant is independent of t.

Step 2. Taking L^2 inner product of (2.1b) with $-\tilde{v}_{xx}$, we deduce

$$\begin{aligned}\frac{1}{2}\frac{\mathrm{d}}{\mathrm{d}t}\|\tilde{v}_x\|^2 + \|\tilde{v}_{xx}\|^2 = &\underbrace{-\int_0^1 (\tilde{u}^2)_x \tilde{v}_{xx}\mathrm{d}x}_{\equiv R_{3a}} + \underbrace{\int_0^1 (\tilde{v}^2)_x \tilde{v}_{xx}\mathrm{d}x}_{\equiv R_{3b}} + \underbrace{2\int_0^1 (\beta\tilde{v})_x \tilde{v}_{xx}\mathrm{d}x}_{\equiv R_{3c}} \\ &+ \underbrace{\int_0^1 (\beta^2)_x \tilde{v}_{xx}\mathrm{d}x}_{\equiv R_{3d}} \underbrace{-2\int_0^1 (\alpha\tilde{u})_x \tilde{v}_{xx}\mathrm{d}x}_{\equiv R_{3e}} \underbrace{-\int_0^1 (\alpha^2)_x \tilde{v}_{xx}\mathrm{d}x}_{\equiv R_{3f}} + \underbrace{\int_0^1 \beta_t \tilde{v}_{xx}\mathrm{d}x}_{\equiv R_{3g}}.\end{aligned} \tag{2.12}$$

Similar to the estimate of R_{2a}, we can show that

$$|R_{3a}| + |R_{3b}| \le C(\|\tilde{u}_x\|^2 + \|\tilde{v}_x\|^2)\|\tilde{v}_{xx}\| \le C(\|\tilde{u}_x\| + \|\tilde{v}_x\|^2)\|\tilde{v}_{xx}\|,$$

where we applied (2.11) for $\|\tilde{u}_x\|^2$. Similar to the estimates of R_{2b} and R_{2c}, we can show that

$$|R_{3c}| + |R_{3e}| \le C(\|\tilde{u}_x\| + \|\tilde{v}_x\|)\|\tilde{v}_{xx}\|.$$

Similar to the estimate of R_{2d}, we can show that

$$|R_{3d}| + |R_{3f}| \le C(|\beta_2 - \beta_1| + |\alpha_2 - \alpha_1|)\|\tilde{v}_{xx}\|.$$

Similar to the estimate of R_{2e}, we can show that

$$|R_{3g}| \le C(|\beta_1'| + |\beta_2'|)\|\tilde{v}_{xx}\|.$$

Substituting the above estimates into (2.12), we can show that

$$\begin{aligned}&\frac{1}{2}\frac{\mathrm{d}}{\mathrm{d}t}\|\tilde{v}_x\|^2 + \frac{1}{2}\|\tilde{v}_{xx}\|^2 \\ &\le C(\|\tilde{v}_x\|^4 + \|\tilde{u}_x\|^2 + \|\tilde{v}_x\|^2 + |\beta_2 - \beta_1| + |\alpha_2 - \alpha_1| + |\beta_1'| + |\beta_2'|).\end{aligned} \tag{2.13}$$

Applying Grönwall's inequality to (2.13) and utilizing Lemma 2.2, we can show that

$$\|\tilde{v}_x(t)\|^2 + \int_0^t \|\tilde{v}_{xx}(\tau)\|^2 \mathrm{d}\tau \le C, \tag{2.14}$$

for some constant which is independent of t. This completes the proof of the lemma. □

2.3. $L_t^\infty H_x^2$–$L_t^2 H_x^3$–Estimates

Lemma 2.4. *Under the assumptions of Theorem* 1.1*, there exists a constant $C > 0$ which is independent of t, such that*

$$\|\tilde{u}_{xx}(t)\|^2 + \|\tilde{v}_{xx}(t)\|^2 + \int_0^t \left(\|\tilde{u}_{xxx}(\tau)\|^2 + \|\tilde{v}_{xxx}(\tau)\|^2\right) \mathrm{d}\tau \le C.$$

Proof. Since the information about the higher order spatial derivatives of the solution is unknown at the boundary points, the usual procedure (differentiating with respect to x) for estimating the $L_t^\infty H_x^2$ and $L_t^2 H_x^3$ norms of the solution can not be directly implemented here. To circumvent such a technical issue, we turn to the estimation of the temporal derivatives of the solution, then utilize the model equations to recover the estimates of the spatial derivatives.

Step 1. Taking ∂_t of (2.1a) and (2.1b), we have

$$\begin{aligned}\tilde{u}_{tt} - (\tilde{u}\tilde{v})_{xt} &= \tilde{u}_{xxt} + \alpha_t\tilde{v}_x + \alpha\tilde{v}_{xt} + \alpha_{xt}\tilde{v} + \alpha_x\tilde{v}_t + \beta_t\tilde{u}_x + \beta\tilde{u}_{xt} + \beta_{xt}\tilde{u} + \beta_x\tilde{u}_t \\ &\quad + \alpha_t\beta_x + \alpha\beta_{xt} + \alpha_{xt}\beta + \alpha_x\beta_t - \alpha_{tt}, \qquad (2.15a)\\ \tilde{v}_{tt} - (\tilde{u}^2)_{xt} &= \tilde{v}_{xxt} - 2\tilde{v}_t\tilde{v}_x - 2\tilde{v}\tilde{v}_{xt} - 2\beta_t\tilde{v}_x - 2\beta\tilde{v}_{xt} - 2\beta_x\tilde{v}_t - 2\beta_{xt}\tilde{v} - 2\beta_t\beta_x \\ &\quad - 2\beta\beta_{xt} + 2\alpha_{xt}\tilde{u} + 2\alpha_x\tilde{u}_t + 2\alpha_t\tilde{u}_x + 2\alpha\tilde{u}_{xt} + 2\alpha_t\alpha_x + 2\alpha\alpha_{xt} - \beta_{tt}. \qquad (2.15b)\end{aligned}$$

Taking L^2 inner product of (2.15a) with $\tilde{u}_t$ and integrating by parts, we can show that

$$\begin{aligned}\frac{1}{2}\frac{\mathrm{d}}{\mathrm{d}t}\|\tilde{u}_t\|^2 + \|\tilde{u}_{xt}\|^2 = &\underbrace{-\int_0^1 (\tilde{u}\tilde{v})_t\tilde{u}_{xt}\mathrm{d}x}_{\equiv R_{4a}} + \underbrace{\int_0^1 \alpha_t\tilde{v}_x\tilde{u}_t\mathrm{d}x}_{\equiv R_{4b}} \underbrace{-\int_0^1 \alpha\tilde{v}_t\tilde{u}_{xt}\mathrm{d}x}_{\equiv R_{4c}} + \underbrace{\int_0^1 \alpha_{xt}\tilde{v}\tilde{u}_t\mathrm{d}x}_{\equiv R_{4d}} \\ &+ \underbrace{\int_0^1 \alpha_x\tilde{v}_t\tilde{u}_t\mathrm{d}x}_{\equiv R_{4e}} + \underbrace{\int_0^1 \beta_t\tilde{u}_x\tilde{u}_t\mathrm{d}x}_{\equiv R_{4f}} + \underbrace{\beta_{xt}\int_0^1 \tilde{u}\tilde{u}_t\mathrm{d}x}_{\equiv R_{4g}} \\ &+ \underbrace{\int_0^1 (\alpha_t\beta_x + \alpha\beta_{xt} + \alpha_{xt}\beta + \alpha_x\beta_t - \alpha_{tt})\tilde{u}_t\mathrm{d}x}_{\equiv R_{4h}} + \frac{\beta_x}{2}\|\tilde{u}_t\|^2. \qquad (2.16)\end{aligned}$$

Using the Sobolev embedding theorem and Lemmas 2.2–2.3, we can show that

$$\begin{aligned}|R_{4a}| &\le \frac{1}{4}\|\tilde{u}_{xt}\|^2 + 2(\|\tilde{u}\|_{L^\infty}^2\|\tilde{v}_t\|^2 + \|\tilde{v}\|_{L^\infty}^2\|\tilde{u}_t\|^2) \\ &\le \frac{1}{4}\|\tilde{u}_{xt}\|^2 + C(\|\tilde{u}\|_{H^1}^2\|\tilde{v}_t\|^2 + \|\tilde{v}\|_{H^1}^2\|\tilde{u}_t\|^2) \\ &\le \frac{1}{4}\|\tilde{u}_{xt}\|^2 + C(\|\tilde{v}_t\|^2 + \|\tilde{u}_t\|^2).\end{aligned}$$

Since $\alpha_t = [\alpha_2'(t) - \alpha_1'(t)]x + \alpha_1'(t)$ is uniformly bounded (see Remark 1.3), we infer that

$$|R_{4b}| \le C(\|\tilde{v}_x\|^2 + \|\tilde{u}_t\|^2).$$

Since α is uniformly bounded, we can show that

$$|R_{4c}| \le \frac{1}{4}\|\tilde{u}_{xt}\|^2 + C\|\tilde{v}_t\|^2.$$

Since $\alpha_{xt} = \alpha_2'(t) - \alpha_1'(t)$ and $\alpha_x = \alpha_2(t) - \alpha_1(t)$ are uniformly bounded, we can show that

$$|R_{4d}| \le C(\|\tilde{v}_x\|^2 + \|\tilde{u}_t\|^2),$$

where we applied Poincaré inequality to $\tilde{v}$, and

$$|R_{4e}| \le C(\|\tilde{v}_t\|^2 + \|\tilde{u}_t\|^2).$$

Similarly, using the uniform boundedness of β_t and β_{xt}, we can show that

$$|R_{4f}| + |R_{4g}| \le C(\|\tilde{u}_x\|^2 + \|\tilde{u}_t\|^2),$$

where we applied Poincaré inequality to $\tilde{u}$. Lastly, R_{4h} is estimated as

$$|R_{4h}| \le (|\alpha_1''| + |\alpha_2''|)\|\tilde{u}_t\|^2 + C(|\alpha_1''| + |\alpha_2''| + |\alpha_1'| + |\alpha_2'| + |\beta_1'| + |\beta_2'| + \|\tilde{u}_t\|^2).$$

Substituting the above estimates into (2.16), we have

$$\begin{aligned}\frac{1}{2}\frac{\mathrm{d}}{\mathrm{d}t}\|\tilde{u}_t\|^2 + \frac{1}{2}\|\tilde{u}_{xt}\|^2 \le (|\alpha_1''| + |\alpha_2''|)\|\tilde{u}_t\|^2 + C(\|\tilde{u}_t\|^2 + \|\tilde{u}_x\|^2 + \|\tilde{v}_t\|^2 + \|\tilde{v}_x\|^2 \\ + |\alpha_1''| + |\alpha_2''| + |\alpha_1'| + |\alpha_2'| + |\beta_1'| + |\beta_2'|).\end{aligned} \tag{2.17}$$

Step 2. Taking L^2 inner product of (2.15b) with $\tilde{v}_t$ and integrating by parts, we can show that

$$\begin{aligned}\frac{1}{2}\frac{\mathrm{d}}{\mathrm{d}t}\|\tilde{v}_t\|^2 + \|\tilde{v}_{xt}\|^2 = -\beta_x\|\tilde{v}_t\|^2 - 2\int_0^1 \tilde{u}\tilde{u}_t\tilde{v}_{xt}\mathrm{d}x + 2\int_0^1 \tilde{v}\tilde{v}_t\tilde{v}_{xt}\mathrm{d}x - 2\int_0^1 \beta_t\tilde{v}_x\tilde{v}_t\mathrm{d}x \\ - 2\beta_{xt}\int_0^1 \tilde{v}\tilde{v}_t\mathrm{d}x + 2\alpha_{xt}\int_0^1 \tilde{u}\tilde{v}_t\mathrm{d}x + 2\int_0^1 \alpha_t\tilde{u}_x\tilde{v}_t\mathrm{d}x - 2\int_0^1 \alpha\tilde{u}_t\tilde{v}_{xt}\mathrm{d}x \\ + \int_0^1 (2\alpha_t\alpha_x + 2\alpha\alpha_{xt} - 2\beta_t\beta_x - 2\beta\beta_{xt} - \beta_{tt})\tilde{v}_t\mathrm{d}x.\end{aligned} \tag{2.18}$$

Using similar arguments as those in deriving the estimates of R_{4a}–R_{4h}, we can show that

$$\begin{aligned}\frac{1}{2}\frac{\mathrm{d}}{\mathrm{d}t}\|\tilde{v}_t\|^2 + \frac{1}{2}\|\tilde{v}_{xt}\|^2 \le (|\beta_1''| + |\beta_2''|)\|\tilde{v}_t\|^2 + C(\|\tilde{u}_t\|^2 + \|\tilde{u}_x\|^2 + \|\tilde{v}_t\|^2 + \|\tilde{v}_x\|^2 \\ + |\beta_1''| + |\beta_2''| + |\beta_1'| + |\beta_2'| + |\alpha_1'| + |\alpha_2'|).\end{aligned} \tag{2.19}$$

Step 3. Using (2.1a) and similar arguments as in **Step 1**, we can show that

$$\begin{aligned}\|\tilde{u}_t\|^2 &\le C(\|(\tilde{u}\tilde{v})_x\|^2 + \|\tilde{u}_{xx}\|^2 + \|(\alpha\tilde{v})_x\|^2 + \|(\beta\tilde{u})_x\|^2 + \|(\alpha\beta)_x\|^2 + \|\alpha_t\|^2) \\ &\le C(\|\tilde{u}_x\|^2 + \|\tilde{v}_x\|^2 + \|\tilde{u}_{xx}\|^2 + |\alpha_1 - \alpha_2| + |\beta_1 - \beta_2| + |\alpha_1'| + |\alpha_2'|).\end{aligned} \tag{2.20}$$

In the same spirit, by using (2.1b), we can show that

$$\|\tilde{v}_t\|^2 \le C(\|\tilde{u}_x\|^2 + \|\tilde{v}_x\|^2 + \|\tilde{v}_{xx}\|^2 + |\alpha_1 - \alpha_2| + |\beta_1 - \beta_2| + |\beta_1'| + |\beta_2'|). \tag{2.21}$$

Using (2.20) and (2.21), we update (2.17) and (2.19) as

$$\frac{1}{2}\frac{\mathrm{d}}{\mathrm{d}t}\|\tilde{u}_t\|^2+\frac{1}{2}\|\tilde{u}_{xt}\|^2\le(|\alpha_1''|+|\alpha_2''|)\|\tilde{u}_t\|^2+C(\|\tilde{u}_{xx}\|^2+\|\tilde{u}_x\|^2+\|\tilde{v}_{xx}\|^2+\|\tilde{v}_x\|^2 \\ +|\alpha_1''|+|\alpha_2''|+|\alpha_1'|+|\alpha_2'|+|\alpha_1-\alpha_2|+|\beta_1'|+|\beta_2'|+|\beta_1-\beta_2|). \tag{2.22}$$

and

$$\frac{1}{2}\frac{\mathrm{d}}{\mathrm{d}t}\|\tilde{v}_t\|^2+\frac{1}{2}\|\tilde{v}_{xt}\|^2\le(|\beta_1''|+|\beta_2''|)\|\tilde{v}_t\|^2+C(\|\tilde{u}_{xx}\|^2+\|\tilde{u}_x\|^2+\|\tilde{v}_{xx}\|^2+\|\tilde{v}_x\|^2 \\ +|\beta_1''|+|\beta_2''|+|\beta_1'|+|\beta_2'|+|\beta_1-\beta_2|+|\alpha_1'|+|\alpha_2'|+|\alpha_1-\alpha_2|). \tag{2.23}$$

Applying Grönwall's inequality to (2.22) and (2.23), using Lemmas 2.2 and 2.3 and the assumptions in Theorem 1.1, we can show that

$$\|\tilde{u}_t(t)\|^2+\|\tilde{v}_t(t)\|^2+\int_0^t\left(\|\tilde{u}_{xt}(\tau)\|^2+\|\tilde{v}_{xt}(\tau)\|^2\right)\mathrm{d}\tau\le C. \tag{2.24}$$

As a consequence of the above estimates, we can show by using (2.1a) and (2.1b) that

$$\|\tilde{u}_{xx}(t)\|^2+\|\tilde{v}_{xx}(t)\|^2+\int_0^t\left(\|\tilde{u}_{xxx}(\tau)\|^2+\|\tilde{v}_{xxx}(\tau)\|^2\right)\mathrm{d}\tau\le C.$$

This completes the proof of Lemma 2.4. □

Lemmas 2.2–2.4 established the desired energy estimates of the solution as stated in Theorem 1.1. The global well-posedness of the initial-boundary value problem thus follows from the local well-posedness in Lemma 2.1, *a priori* estimates in Lemmas 2.2–2.4 and standard continuation argument. To complete the proof of Theorem 1.1, it remains to derive the temporal decaying of the perturbed variables, which is carried out in the next subsection.

2.4. Decay estimate

We first recall a technical lemma which is essential in deriving the temporal decaying of the perturbations. The proof of the lemma can be found in [53].

Lemma 2.5. *Let $f\in W^{1,1}(0,\infty)$ be a nonnegative function. Then $f(t)\to 0$ as $t\to\infty$.*

Using Lemma 2.5, we can show the following:

Lemma 2.6. *Under the assumptions of Theorem* 1.1, $\|\tilde{u}(t)\|_{H^2}^2+\|\tilde{v}(t)\|_{H^2}^2\to 0$, *as* $t\to\infty$.

Proof. **Step 1.** Based on Lemma 2.2, we know that

$$\|\tilde{u}_x(t)\|^2+\|\tilde{v}_x(t)\|^2\in L^1((0,\infty)), \tag{2.25}$$

which, together with Poincaré inequality, implies

$$\|\tilde{u}(t)\|^2+\|\tilde{v}(t)\|^2\in L^1((0,\infty)). \tag{2.26}$$

Using the assumptions of Theorem 1.1 and the energy estimates established in Lemmas 2.2–2.4, we can deduce from (2.6) and (2.7) that

$$\Big|\frac{\mathrm{d}}{\mathrm{d}t}\Big(\|\tilde{u}\|^2+\frac{1}{2}\|\tilde{v}\|^2\Big)\Big| \le C(\|\tilde{u}_x\|^2+\|\tilde{v}_x\|^2+|\alpha_2-\alpha_1|+|\alpha_2'|+|\alpha_1'|+|\beta_2-\beta_1|+|\beta_2'|+|\beta_1'|),$$

where the constant is independent of t. Integrating the above inequality, we obtain

$$\frac{\mathrm{d}}{\mathrm{d}t}\Big(\|\tilde{u}(t)\|^2+\frac{1}{2}\|\tilde{v}(t)\|^2\Big) \in L^1((0,\infty)). \tag{2.27}$$

Collectively, (2.26) and (2.27) imply

$$\Big(\|\tilde{u}(t)\|^2+\frac{1}{2}\|\tilde{v}(t)\|^2\Big) \in W^{1,1}((0,\infty)).$$

Hence, $\|\tilde{u}(t)\|^2+\|\tilde{v}(t)\|^2 \to 0$, as $t\to\infty$, according to Lemma 2.5. Moreover, since $\|\tilde{u}_{xx}(t)\|$ and $\|\tilde{v}_{xx}(t)\|$ are uniformly bounded with respect to time, the decaying of $\|\tilde{u}_x(t)\|^2+\|\tilde{v}_x(t)\|^2$ follows from the decaying of $\|\tilde{u}(t)\|^2+\|\tilde{v}(t)\|^2$ and the interpolation inequality $\|f_x\|^2 \le \|f\|\cdot\|f_{xx}\|$, for any $f\in H_0^2((0,1))$.

Step 2. For the second order spatial derivatives, we know from (2.24) and Poincaré inequality that

$$\|\tilde{u}_t(t)\|^2+\|\tilde{v}_t(t)\|^2 \in L^1((0,\infty)).$$

Based on (2.17), (2.19), and previous estimates, it can be shown that

$$\begin{aligned}\Big|\frac{\mathrm{d}}{\mathrm{d}t}\left(\|\tilde{u}_t\|^2+\|\tilde{v}_t\|^2\right)\Big| \le{}& C(\|\tilde{u}_t\|^2+\|\tilde{v}_t\|^2+\|\tilde{u}_{xt}\|^2+\|\tilde{v}_{xt}\|^2+\|\tilde{u}_x\|^2+\|\tilde{v}_x\|^2\\ &+|\alpha_1''|+|\alpha_2''|+|\alpha_1'|+|\alpha_2'|+|\beta_1''|+|\beta_2''|+|\beta_1'|+|\beta_2'|),\end{aligned}$$

which implies

$$\frac{\mathrm{d}}{\mathrm{d}t}\left(\|\tilde{u}_t(t)\|^2+\|\tilde{v}_t(t)\|^2\right) \in L^1((0,\infty)).$$

Hence, $\|\tilde{u}_t(t)\|^2+\|\tilde{v}_t(t)\|^2 \in W^{1,1}((0,\infty))$, and thus $\|\tilde{u}_t(t)\|^2+\|\tilde{v}_t(t)\|^2\to 0$, as $t\to\infty$. Using (2.1), we can show that

$$\begin{aligned}\|\tilde{u}_{xx}\|^2+\|\tilde{v}_{xx}\|^2 \le{}& C(\|\tilde{u}_t\|^2+\|\tilde{v}_t\|^2+\|\tilde{u}_x\|^2+\|\tilde{v}_x\|^2\\ &+|\alpha_1-\alpha_2|+|\alpha_1'|+|\alpha_2'|+|\beta_1-\beta_2|+|\beta_1'|+|\beta_2'|).\end{aligned} \tag{2.28}$$

Since $\alpha_1-\alpha_2$, α_1, α_2, $\beta_1-\beta_2$, β_1' and β_2' belong to $W^{1,1}((0,\infty))$, they tend to zero as $t\to\infty$. Therefore, the decaying of $\|\tilde{u}_{xx}(t)\|^2+\|\tilde{v}_{xx}(t)\|^2$ follows from (2.28) and the decaying of the first order derivatives of the perturbed solution. This completes the proof of Lemma 2.6. □

Collectively, Theorem 1.1 follows from Lemmas 2.1–2.4 and 2.6.

3. Numerical experiments

We have shown that large data classical solutions to an initial boundary value problem of the nonlinear PDE system (1.10), subject to unmatched Dirichlet type dynamic boundary conditions, stabilize in the long run under appropriate assumptions on the boundary data. However, it was mentioned in Remark 1.2 that the technical assumptions in Theorem 1.1 imply the unmatched boundary data will eventually match at the endpoints, i.e., the final states are constants. This indeed rules out the more physically/biologically relevant situations in which the final equilibria are non-trivial. Another situation that is not covered by Theorem 1.1 is when the boundary data are time periodic. Because of the ubiquitous presence of time periodic phenomena in natural sciences, it is worth investigating whether time periodic boundary data generate time periodic solutions of the nonlinear PDE model. Moreover, our theoretical result only included the special case $\gamma = 2$. It is not clear whether the results hold true for other values of γ, especially when γ is a fraction. Inspired by these observations, we devote the last part of this paper to numerically showcasing two problems that are not covered by the analytical results. These include dynamic boundary data with unmatched final states and time periodic boundary conditions. We use a finite difference scheme to simulate the problems. We hope that our numerical studies will shed some light on, and provide guidance for further analytical studies in this specific area of research.

Recall the initial-boundary value problem

$$\begin{aligned}
&u_t - (uv)_x = u_{xx}, && x \in (0,1), \quad t > 0,\\
&v_t - (u^\gamma)_x = v_{xx} - (v^2)_x, && x \in (0,1), \quad t > 0,\\
&(u,v)(x,0) = (u_0, v_0)(x), && x \in [0,1],\\
&u(0,t) = \alpha_1(t), \quad u(1,t) = \alpha_2(t), && t \geq 0,\\
&v(0,t) = \beta_1(t), \quad v(1,t) = \beta_2(t), && t \geq 0.
\end{aligned}$$

where the initial and boundary data are compatible, i.e.,

$$u_0(0) = \alpha_1(0), \quad u_0(1) = \alpha_2(0), \quad v_0(0) = \beta_1(0), \quad v_0(1) = \beta_2(0).$$

3.1. Dynamic boundary data with unmatched final states

In Example 1, we set $u_0 = 5\sin(\pi x/2) + 10$, $v_0 = 2 + \cos(\pi x/2)$, $\alpha_1(t) = 9 + \frac{1}{1+t}$, $\alpha_2(t) = 14 + e^{-t}$, $\beta_1(t) = 4 - e^{-t}$, $\beta_2(t) = 2 + \frac{t}{1+t}$. The value of γ is set as γ =1.5, 2 and 2.5. The numerical solutions of u and v evolve to non-trivial steady states as shown in Figure 1.

Meanwhile, it is interesting to observe from Figure 2 that the graphs of the steady state solutions steepen near the boundary points as γ increases. We thus expect boundary layers will develop near the endpoints of the interval as γ grows. Mathematical analysis of this problem requires more sophisticated tools and we leave the investigation in a future paper.

3.2. Time-Periodic boundary conditions

In Examples 2A, 2B and 2C, we simulate the problem by using time-periodic boundary data. The simulations are run for the same values of γ as in Example 1. It turns out, however, the simulation

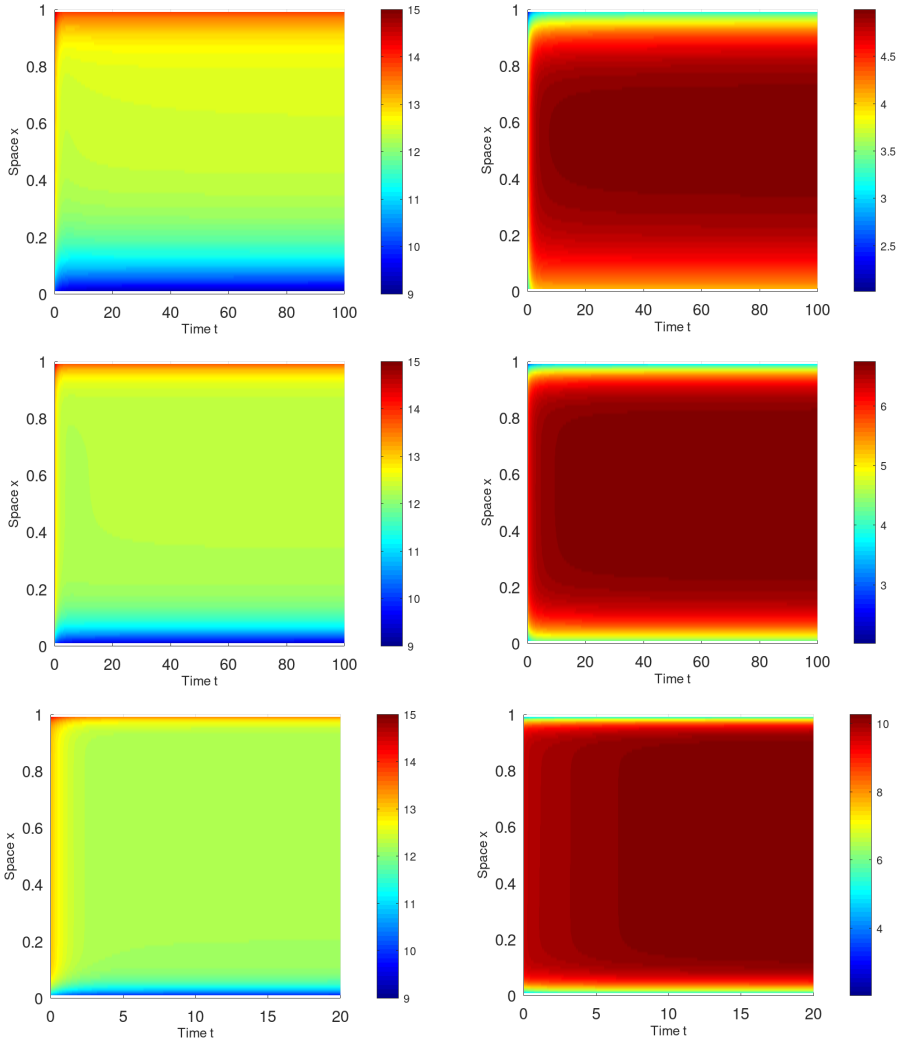

Figure 1. Example 1. First row: $\gamma = 1.5$. Second row: $\gamma = 2$. Third row: $\gamma = 2.5$. Left column: u. Right column: v.

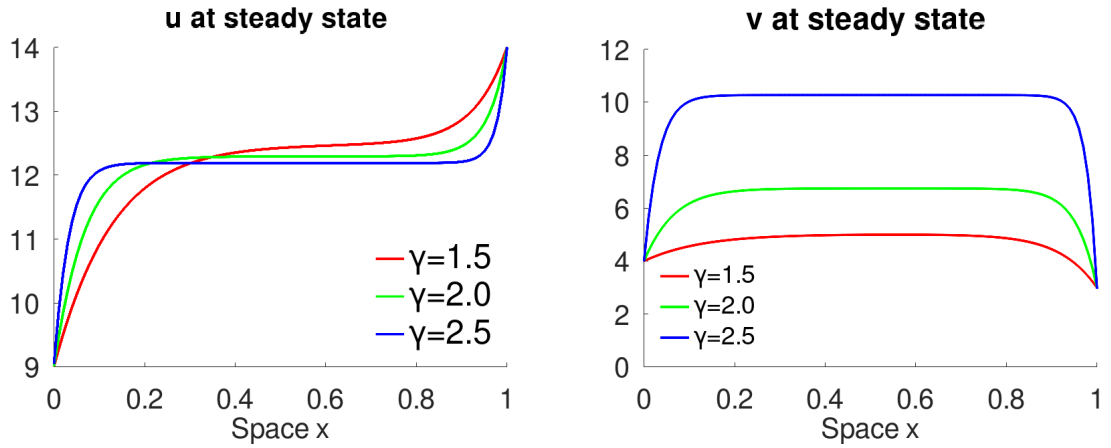

Figure 2. Profiles of steady state solutions in Example 1.

results are almost the same for different values of γ and the plots are visibly indistinguishable. The plots presented below are for $\gamma = 1.5$.

In Example 1A, the initial values are $u_0 = 2+x(1-x)$ and $v_0 = 4+\sin(2\pi x)$. The boundary conditions are $\alpha_1(t) = \alpha_2(t) = 2 + \sin(2\pi t)$ and $\beta_1(t) = \beta_2(t) = 4 + \sin(2\pi t)$. Thus the boundary conditions of u and v have the same period and same phase angle. The solutions are shown in Figure 3, where both u and v evolve to periodic solutions at later time, although initially they are not. Note the maximum and minimum values of u and v occur at the same time.

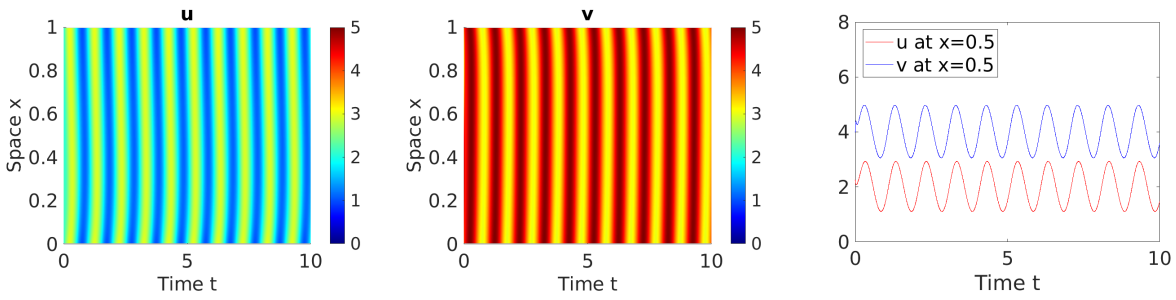

Figure 3. Example 2A. The last panel shows the evolution of u and v at $x = 0.5$.

In Example 2B, the initial values of u and v are the same as those in Example 2A. The boundary condition of u is still $\alpha_1(t) = \alpha_2(t) = 2+\sin(2\pi t)$, but that of v is changed to $\beta_1(t) = \beta_2(t) = 3+\cos(2\pi t)$. That is, they share the same period but have different phase angles. The solutions are shown in Figure 4, where both u and v evolve to periodic solutions. Note the maximum and minimum values of u and v occur at a gap of $1/4$ time units, which originates from the difference of the phase angles of α and β.

In Example 2C, the initial values of u and v are the same as in Examples 2A and 2B. The boundary condition of u is changed to $\alpha_1(t) = 2 + \sin(2\pi t)$ and $\alpha_2(t) = 1 + \cos(2\pi t)$, and that of v is changed to $\beta_1(t) = 4 + \sin(2\pi t)$ and $\beta_2(t) = 3 + \cos(2\pi t)$. That is, the left boundary conditions for u and v have

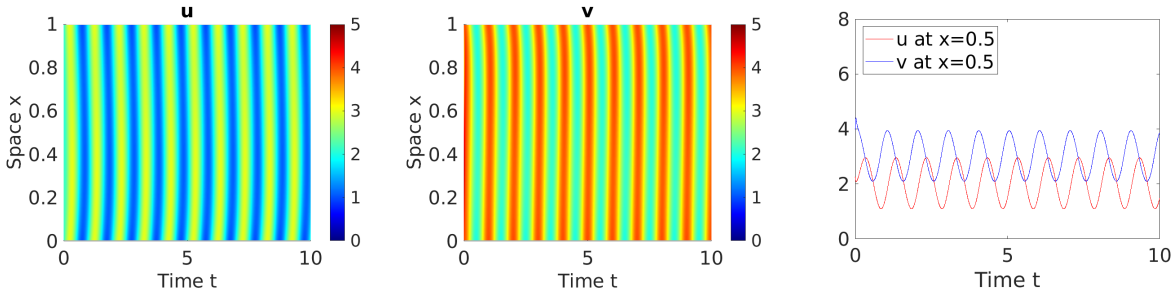

Figure 4. Example 2B. The last panel shows the evolution of u and v at $x = 0.5$.

the same phase angle and the right boundary conditions have another phase angle. The solutions are shown in Figure 5, where both u and v evolve to periodic solutions.

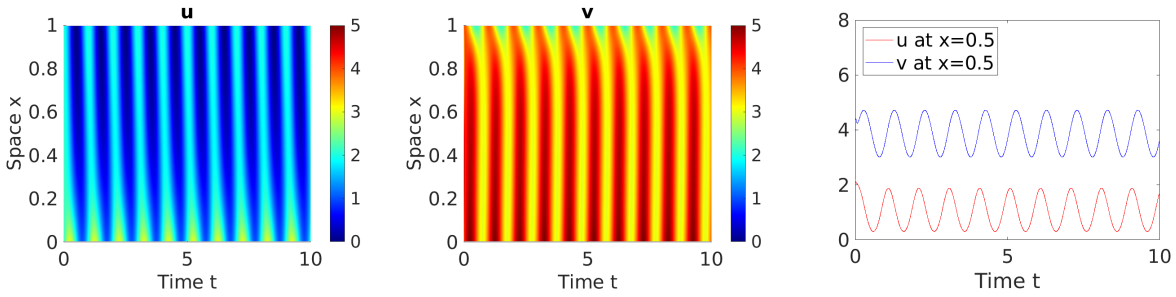

Figure 5. Example 2C. The last panel shows the evolution of u and v at $x = 0.5$.

4. Conclusions

In this paper, we studied the global dynamics of classical solutions to the nonlinear PDE system (1.1) subject to dynamic boundary conditions. When $\gamma = 2$, we proved that if the time-dependent Dirichlet-type boundary conditions satisfy (1.13)–(1.15), there exists a unique global-in-time solution to the initial-boundary value problem (IBVP) for any initial data in $H^2((0, 1))$, and the solution is shown to converge asymptotically to the steady state determined by the boundary data as time goes to infinity. In our analytical results, the boundary values of the solution are not required to match at any time. This generalized the previous work [52], where the boundary values must match for all time. To investigate some problems that are not covered by our analytical results, we numerically simulated the IBVP for dynamic boundary conditions with unmatched end-states or periodic in time. Our numerical results suggested that in the former case, the solution converges to a non-trivial steady state in the long run, and in the latter case, time periodicity was observed in the solution after certain duration of time. Moreover, we simulated the problem for several values of γ different from 2 and discovered the phenomenon of boundary steepening of the steady state as the value of γ increases. Rigorous mathematical studies of these phenomena will be carried out in future works.

Acknowledgments

The authors would like to thank the anonymous referees for their valuable comments and suggestions which help substantially improve the quality of the paper. Support for this work came in part from a National Natural Science Foundation of China Award 12171116 (LX), a Fundamental Research Funds for Central Universities of China Award 3072020CFT2402 (LX), and from Simons Foundation Collaboration Grant for Mathematicians Award 413028 (KZ).

Conflict of interest

The authors declare that there is no conflict of interest.

References

1. J. D. Murray, *Mathematical Biology I: An Introduction*, 3rd edition, Springer-Verlag, New York, 2002. https://doi.org/10.1023/A:1022616217603
2. R. Tyson, S. R. Lubkin, J. D. Murray, Model and analysis of chemotactic bacterial patterns in a liquid medium, *J. Math. Biol.*, **38** (1999), 359–375. https://doi.org/10.1007/s002850050153
3. A. Gamba, D. Ambrosi, A. Coniglio, A. de Candia, S. Di Talia, E. Giraudo, et al., Percolation, morphogenesis, and Burgers dynamics in blood vessels formation, *Phys. Rev. Lett.*, **90** (2003), 118101. https://doi.org/10.1103/PhysRevLett.90.118101
4. K. J. Painter, P. K. Maini, H. G. Othmer, Stripe formation in juvenile pomacanthus explained by a generalized Turing mechanism, *Proc. Nat. Acad. Sci.*, **96** (1999), 5549–5554. https://doi.org/10.1073/pnas.96.10.5549
5. M. A. J. Chaplain, A. M. Stuart, A model mechanism for the chemotactic response of endothelial cells to tumor angiogenesis factor, *IMA J. Math. Appl. Med.*, **10** (1993), 149–168. https://doi.org/10.1093/imammb/10.3.149
6. K. J. Painter, P. K. Maini, H. G. Othmer, A chemotactic model for the advance and retreat of the primitive streak in avian development, *Bull. Math. Biol.*, **62** (2000), 501–525. https://doi.org/10.1006/bulm.1999.0166
7. H. Höfer, J. A. Sherratt, P. K. Maini, Cellular pattern formation during Dictyostelium aggregation, *Phys. D*, **85** (1995), 425–444. https://doi.org/10.1016/0167-2789(95)00075-F
8. G. J. Petter, H. M. Byrne, D. L. S. McElwain, J. Norbury, A model of wound healing and angiogenesis in soft tissue, *Math. Biosci.*, **136** (2003), 35–63. https://doi.org/10.1016/0025-5564(96)00044-2
9. C. S. Patlak, Random walk with persistence and external bias, *Bull. Math. Biophys.*, **15** (1953), 311–338. https://doi.org/10.1007/BF02476407
10. E. F. Keller, L. A. Segel, Initiation of slime mold aggregation viewed as an instability, *J. Theor. Biol.*, **26** (1970), 399–415. https://doi.org/10.1016/0022-5193(70)90092-5

11. E. F. Keller, L. A. Segel, Model for chemotaxis, *J. Theor. Biol.*, **30** (1971), 225–234. https://doi.org/10.1016/0022-5193(71)90050-6
12. E. F. Keller, L. A. Segel, Traveling bands of chemotactic bacteria: a theoretical analysis, *J. Theor. Biol.*, **26** (1971), 235–248. https://doi.org/10.1016/0022-5193(71)90051-8
13. N. Bellomo, A. Bellouquid, Y. Tao, M. Winkler, Toward a mathematical theory of Keller-Segel models of pattern formation in biological tissues, *Math. Models Methods Appl. Sci.*, **25** (2015), 1663–1763. https://doi.org/10.1142/S021820251550044X
14. T. Hillen, K. Painter, A users guide to PDE models for chemotaxis, *J. Math. Biol.*, **58** (2009), 183–217. https://doi.org/10.1007/s00285-008-0201-3
15. D. Horstmann, From 1970 until present: The Keller-Segel model in chemotaxis and its consequences I, *Jahresber. Dtsch. Math. Ver.*, **105** (2003), 103–165.
16. J. Adler, Chemotaxis in bacteria, *Science*, **153** (1966), 708–716. https://doi.org/10.1126/science.153.3737.708
17. W. Alt, D. A. Lauffenburger, Transient behavior of a chemotaxis system modeling certain types of tissue inflammation, *J. Math. Biol.*, **24** (1987), 691–722. https://doi.org/10.1007/BF00275511
18. D. Balding, D. L. S. McElwain, A mathematical model of tumour-induced capillary growth, *J. Theor. Biol.*, **114** (1985), 53–73. https://doi.org/10.1016/S0022-5193(85)80255-1
19. F. W. Dahlquist, P. Lovely, D. E. Jr Koshland, Quantitative analysis of bacterial migration in chemotaxis, *Nat. New Biol.*, **236** (1972), 120–123. https://doi.org/10.1038/newbio236120a0
20. Y. V. Kalinin, L. Jiang, Y. Tu, M. Wu, Logarithmic sensing in Escherichia coli bacterial chemotaxis, *Bio. J.*, **96** (2009), 2439–2448. https://doi.org/10.1016/j.bpj.2008.10.027
21. H. A. Levine, B. D. Sleeman, A system of reaction diffusion equations arising in the theory of reinforced random walks, *SIAM J. Appl. Math.*, **57** (1997), 683–730. https://doi.org/10.1137/S0036139995291106
22. H. Othmer, A. Stevens, Aggregation, blowup and collapse: The ABC's of taxis in reinforced random walks, *SIAM J. Appl. Math.*, **57** (1997), 1044–1081. https://doi.org/10.1137/S0036139995288976
23. H. A. Levine, B. D. Sleeman, M. Nilsen-Hamilton, A mathematical model for the roles of pericytes and macrophages in the initiation of angiogenesis. i. the role of protease inhibitors, *Math. Biosci.*, **168** (2000), 77–115. https://doi.org/10.1016/S0025-5564(00)00034-1
24. M. A. Fontelos, A. Friedman, B. Hu, Mathematical analysis of a model for the initiation of angiogenesis, *SIAM J. Math. Anal.*, **33** (2002), 1330–1355. https://doi.org/10.1137/S0036141001385046
25. J. Guo, J. Xiao, H. Zhao, C. Zhu, Global solutions to a hyperbolic-parabolic coupled system with large initial data, *Acta Math. Sci. Ser. B (Engl. Ed.)*, **29** (2009), 629–641. https://doi.org/10.1016/S0252-9602(09)60059-X

26. Q. Hou, C. Liu, Y. Wang, Z. A. Wang, Stability of boundary layers for a viscous hyperbolic system arising from chemotaxis: one dimensional case, *SIAM J. Math. Anal.*, **50** (2018), 3058–3091. https://doi.org/10.1137/17M112748X

27. Q. Hou, Z. A. Wang, Convergence of boundary layers for the Keller-Segel system with singular sensitivity in the half-plane, *J. Math. Pures. Appl.*, **130** (2019), 251–287. https://doi.org/10.1016/j.matpur.2019.01.008

28. Q. Hou, Z. A. Wang, K. Zhao, Boundary layer problem on a hyperbolic system arising from chemotaxis, *J. Differ. Equations*, **261** (2016), 5035–5070. https://doi.org/10.1016/j.jde.2016.07.018

29. D. Li, R. Pan, K. Zhao, Quantitative decay of a one-dimensional hybrid chemotaxis model with large data, *Nonlinearity*, **28** (2015), 2181–2210. https://doi.org/10.1088/0951-7715/28/7/2181

30. H. Li, K. Zhao, Initial-boundary value problems for a system of hyperbolic balance laws arising from chemotaxis, *J. Differ. Equations*, **258** (2015), 302–338. https://doi.org/10.1016/j.jde.2014.09.014

31. T. Li, R. Pan, K. Zhao, Global dynamics of a hyperbolic-parabolic model arising from chemotaxis, *SIAM J. Appl. Math.*, **72** (2012), 417–443. https://doi.org/10.1137/110829453

32. V. R. Martinez, Z. A. Wang, K. Zhao, Asymptotic and viscous stability of large-amplitude solutions of a hyperbolic system arising from biology, *Indiana Univ. Math. J.*, **67** (2018), 1383–1424. https://www.jstor.org/stable/45010333

33. H. Peng, Z. A. Wang, K. Zhao, C. Zhu, Boundary layers and stabilization of the singular Keller-Segel model, *Kinet. Relat. Models*, **11** (2018), 1085–1123. https://doi.org/10.3934/krm.2018042

34. Y. Tao, L. Wang, Z. A. Wang, Large-time behavior of a parabolic-parabolic chemotaxis model with logarithmic sensitivity in one dimension, *Disc. Cont. Dyn. Syst., Ser. B*, **18** (2013), 821–845. https://doi.org/10.3934/dcdsb.2013.18.821

35. Z. A. Wang, K. Zhao, Global dynamics and diffusion limit of a parabolic system arising from repulsive chemotaxis, *Commun. Pure Appl. Anal.*, **12** (2013), 3027–3046. https://doi.org/10.3934/cpaa.2013.12.3027

36. K. Choi, M. Kang, Y. Kwon, A. Vasseur, Contraction for large perturbations of traveling waves in a hyperbolic-parabolic system arising from a chemotaxis model, *Math. Models Methods Appl. Sci.*, **30** (2020), 387–437. https://doi.org/10.1142/S0218202520500104

37. H. Jin, J. Li, Z. A. Wang, Asymptotic stability of traveling waves of a chemotaxis model with singular sensitivity, *J. Differ. Equations*, **255** (2013), 193–219. https://doi.org/10.1016/j.jde.2013.04.002

38. J. Li. T. Li, Z. A. Wang, Stability of traveling waves of the Keller-Segel system with logarithmic sensitivity, *Math. Models Methods Appl. Sci.*, **24** (2014), 2819–2849. https://doi.org/10.1142/S0218202514500389

39. T. Li, Z. A. Wang, Nonlinear stability of traveling waves to a hyperbolic-parabolic system modeling chemotaxis, *SIAM J. Appl. Math.*, **7** (2009), 1522–1541. https://doi.org/10.1137/09075161X

40. T. Li, Z. A. Wang, Nonlinear stability of large amplitude viscous shock waves of a generalized hyperbolic-parabolic system arising in chemotaxis, *Math. Models Methods Appl. Sci.*, **20** (2010), 1967–1998. https://doi.org/10.1142/S0218202510004830

41. T. Li, Z. A. Wang, Asymptotic nonlinear stability of traveling waves to conservation laws arising from chemotaxis, *J. Differ. Equations*, **250** (2011), 1310–1333. https://doi.org/10.1016/j.jde.2010.09.020

42. T. Li, Z. A. Wang, Steadily propagating waves of a chemotaxis model, *Math. Biosci.*, **240** (2012), 161–168. https://doi.org/10.1016/j.mbs.2012.07.003

43. H. Peng, Z. A. Wang, Nonlinear stability of strong traveling waves for the singular Keller-Segel system with large perturbations, *J. Differ. Equations*, **265** (2018), 2577–2613. https://doi.org/10.1016/j.jde.2018.04.041

44. Z. A. Wang, Mathematics of traveling waves in chemotaxis, *Disc. Cont. Dyn. Syst. Ser. B*, **18** (2013), 601–641. https://doi.org/10.3934/dcdsb.2013.18.601

45. J. A. Carrillo, J. Li, Z. A. Wang, Boundary spike-layer solutions of the singular Keller–Segel system: existence and stability, *Proc. London Math. Soc.*, **122** (2021), 42–68. https://doi.org/10.1112/plms.12319

46. R. M. Fuster-Aguilera, V. R. Martinez, K. Zhao, A PDE model for chemotaxis with logarithmic sensitivity and logistic growth, preprint, arXiv:2012.10521.

47. Y. Zeng, Nonlinear stability of diffusive contact wave for a chemotaxis model, *J. Differ. Equations*, **308** (2022), 286–326. https://doi.org/10.1016/j.jde.2021.11.008

48. Y. Zeng, K. Zhao, On the Logarithmic Keller-Segel-Fisher/KPP System, *Disc. Cont. Dyn. Syst.*, **39** (2019), 5365–5402. https://doi.org/10.3934/dcds.2019220

49. Y. Zeng, K. Zhao, Optimal decay rates for a chemotaxis model with logistic growth, logarithmic sensitivity and density-dependent production/consumption rate, *J. Differ. Equations*, **268** (2020), 1379–1411. https://doi.org/10.1016/j.jde.2019.08.050

50. Y. Zeng, K. Zhao, Optimal decay rates for a chemotaxis model with logistic growth, logarithmic sensitivity and density-dependent production/consumption rate, *J. Differ. Equations*, **29** (2020), 6359–6363. https://doi.org/10.1016/j.jde.2019.08.050

51. Y. Zeng, K. Zhao, Asymptotic behavior of solutions to a chemotaxis-logistic model with transitional end-states, *J. Differ. Equations*, **336** (2022), 1–43. https://doi.org/10.1016/j.jde.2022.07.013

52. Z. Feng, J. Xu, L. Xue, K. Zhao, Initial and boundary value problem for a system of balance laws from chemotaxis: Global dynamics and diffusivity limit, *Ann. Appl. Math.*, **37** (2021), 61–110. https://doi.org/10.4208/aam.OA-2020-0004

53. N. Zhu, Z. Liu, V. R. Martinez, K. Zhao, Global Cauchy problem of a system of parabolic conservation laws arising from a Keller-Segel type chemotaxis model, *SIAM J. Math. Anal.*, **50** (2018), 5380–5425. https://doi.org/10.1137/17M1135645

54. N. Zhu, Z. Liu, F. Wang, K. Zhao, Asymptotic dynamics of a system of conservation laws from chemotaxis, *Disc. Cont. Dyn. Syst.*, **41** (2021), 813–847. https://doi.org/10.3934/dcds.2020301

55. F. Wang, L. Xue, K. Zhao, X. Zheng, Global stabilization and boundary control of generalized Fisher/KPP equation and application to diffusive SIS model, *J. Differ. Equations*, **275** (2021), 391–417. https://doi.org/10.1016/j.jde.2020.11.031

AIMS Press